THE RADICAL CATION OF BACTERIOCHLOROPHYLL b.
A LIQUID-PHASE ENDOR AND TRIPLE RESONANCE STUDY

F. LENDZIAN [a], W. LUBITZ [b], R. STEINER [c], E. TRÄNKLE [d],
M. PLATO [a], H. SCHEER [c] and K. MÖBIUS [a]

[a] *Institut für Molekülphysik, Freie Universität Berlin, D-1000 Berlin 33, West Germany*
[b] *Institut für Organische Chemie, Freie Universität Berlin, D-1000 Berlin 33, West Germany*
[c] *Institut für Botanik, Universität München, D-8000 Munich 19, West Germany*
[d] *Institut für Theorie der Elementarteilchen, Freie Universität Berlin, D-1000 Berlin 33, West Germany*

The radical cation of bacteriochlorophyll b (BChl b) is investigated by ENDOR and TRIPLE resonance in liquid solution. The experimental hyperfine coupling constants, ten proton and three nitrogen couplings, are compared with the predictions from advanced molecular-orbital calculations (RHF INDO/SP). The detailed picture obtained of the spin density distribution is a prerequisite for the investigation of the primary electron donor radical cation in BChl b containing photosynthetic bacteria.

1. Introduction

The primary processes of photosynthesis involve light-induced charge separation followed by fast electron transfer reactions [1,2]. These reactions take place in the reaction centre (RC), a protein complex [3]. In photosynthetic bacteria the participating molecules are bacteriochlorophylls (BChl), bacteriopheophytins and quinones which are all embedded in the protein matrix [1–3]. For a complete understanding of the primary processes a detailed knowledge about the spatial and electronic structure of these molecules in their ground, excited, and charged radical states is indispensable [3–6].

For the RC of the bacterium *Rhodopseudomonas* (*Rps.*) *viridis* which has recently been crystallized [7], the spatial arrangement of the pigment molecules has been determined by X-ray diffraction [8]. One of the important results of this work is the finding of a bacteriochlorophyll dimer. Such a dimer had been proposed originally for the primary electron donor P on the basis of EPR experiments on $P^{\ddagger}$ and BChl $a^{\ddagger}$. [9]. It has been confirmed later by ENDOR experiments in frozen [10,11] and liquid [12–14] RC solutions. Since so far *Rps. viridis* is the only organism for which an X-ray structure analysis of the RC was

performed, other approaches for the structural characterization of the RC are desirable. For the paramagnetic molecules high-resolution liquid-phase ENDOR in combination with advanced MO calculations represent such an approach [14–16]. The basic procedure is first to elucidate in detail the spin density distribution for the involved molecules in vitro and in vivo [12–14]. These will then be compared with the results of advanced MO calculations for various possible molecular structures. Criteria for highly probable configurations are the agreement between experimental and theoretical spin densities and the total energy of the system [15]. This method has been applied to the primary electron donor radical cation $P^{\ddagger}$ of BChl a containing bacteria (*Rps. sphaeroides* and *Rhodospirillum rubrum*) yielding detailed structural proposals [14–16]. Similar investigations of *Rps. viridis* are particularly important because they directly show whether this procedure gives structural information consistent with an X-ray analysis. Structural information from ENDOR combined with MO theory is of course obtained less directly than that from an X-ray analysis and may be hampered by the problem of uniqueness [15]. However, a great advantage of this method is that single-crystal samples are not required. Primarily the ENDOR experiments

measure the spatial distribution of the unpaired electron, information which is important for the understanding of electron-transfer processes and which is not obtainable from X-ray data.

Clearly, a detailed investigation of in vitro BChl b^+ is prerequisite for the comparison with the in vivo system. BChl b is chemically very unstable and decomposes rapidly in the presence of light and oxygen [17,18]. A rapid decomposition of this bacteriochlorin to products of the chlorin type has also been reported for its radical cation [19]. As a consequence ENDOR experiments have so far been performed on this radical in *frozen solution* where only part of the hyperfine structure could be resolved [19]. Here, we present a high-resolution electron spin density map for BChl b^+ obtained from *liquid solution* ENDOR and TRIPLE resonance that agrees well with the results from advanced MO calculations.

2. Materials and methods

BChl b was isolated from *Rps. viridis* after a modified method of Strain and Svec [20]. The crude pigment mixture was purified by sucrose chromatography in dim green light. The used solvents as well as the column were saturated with nitrogen and the solvent reservoirs were kept over magnesium hydroxicarbonate and sodium ascorbate. The isolated BChl b was stored under argon below $-20°C$ in the dark.

The radical cation of BChl b was generated by oxidation with zinc tetraphenylporphin perchlorate $(ZnTPP^+ClO_4^-)$. An excess of BChl b was used to avoid any contributions of the ZnTPP radical cation to the EPR and ENDOR spectra of BChl b^+.

In order to avoid further oxidation and isomerization reactions of BChl b [18,19] the preparation has been carried out in the sample tube inside the ENDOR cavity at $T = 220$ K in the dark under argon atmosphere. The sample tube was then closed and the EPR and ENDOR measurements were performed immediately. Under these conditions, the lifetime of the BChl b radical cation was about half an hour.

The laboratory-built ENDOR and TRIPLE spectrometer has been described [21,22]. For a discussion of the potential advantages of the electron—nuclear—nuclear triple resonance methods both "special TRIPLE" and "general TRIPLE", the reader is referred to refs. [23,24].

s-spin densities and total energies for geometry optimization were calculated by a restricted Hartree—Fock procedure for doublet states ("half-electron method" by Dewar [25]) using the INDO approximation and parameterization by Pople and Beveridge [26] and a subsequent perturbation treatment of spin polarization effects (RHF INDO/SP method) [15]. The calculations were performed on a CRAY-1M vector computer of the Konrad Zuse Computer Center of Berlin.

3. Results and discussion

The first derivative EPR spectrum of BChl b^+ (fig. 2) consists of a Gaussian line showing no resolved hyperfine structure. The g value (2.0025 ± 0.0001) is in accordance with earlier results [19]. There is a
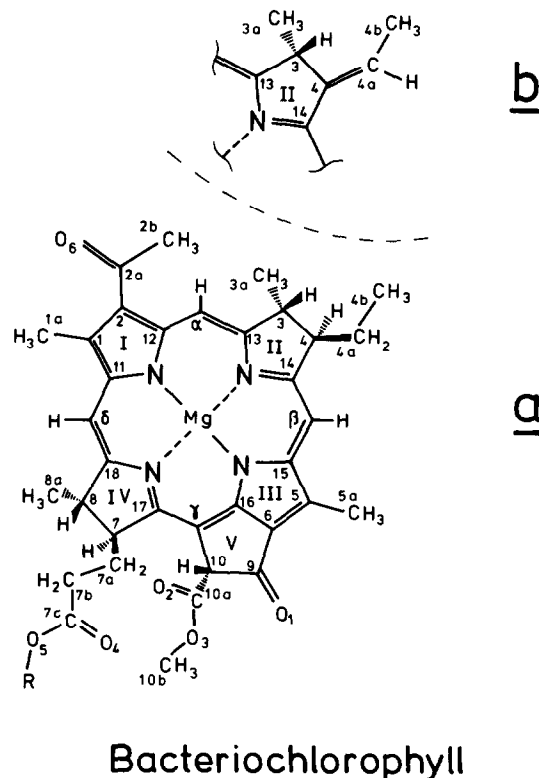

Bacteriochlorophyll

Fig. 1. Molecular structures and numbering scheme of bacteriochlorophyll a (BChl a) and BChl b. The ethyl group and the proton at position 4 (ring II) in BChl a are replaced by an ethylidene group in BChl b. R = phytyl ($C_{20}H_{39}$).

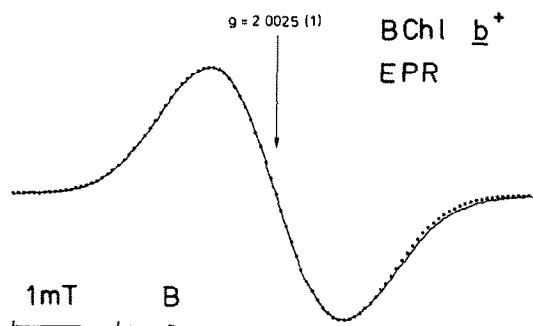Fig. 2. EPR spectrum of BChl b$^+$ in CH_2Cl_2/CH_3OH (6:1). Solid line: T = 215 K (liquid solution); linewidth: 1.26 ± 0.02 mT (T = 215 K); in frozen solution (T = 145 K, spectrum not shown) the linewidth is significantly larger (1.35 ± 0.02 mT), see text. Dotted line: simulation using the isotropic proton and nitrogen hfcs and the assignments given in table 1.
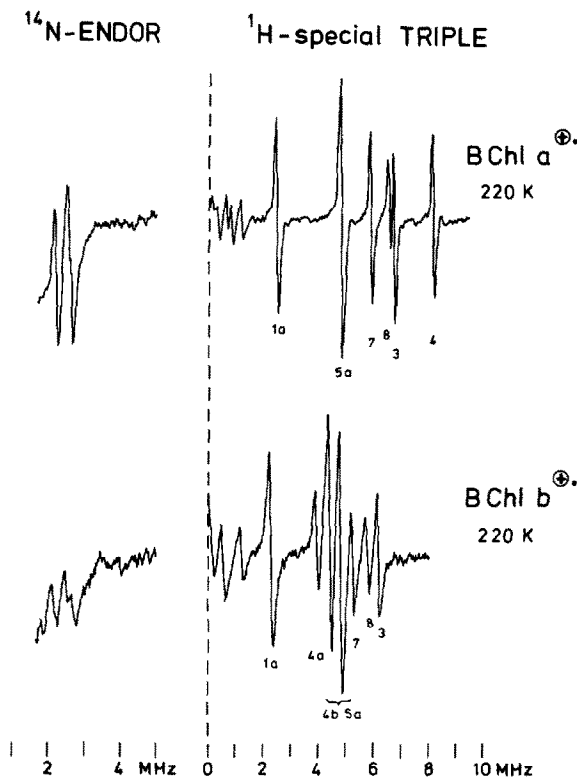

Fig. 3. High-frequency ^{14}N-ENDOR lines (^{14}N Larmor frequency 1.04 MHz) and proton special TRIPLE spectra of BChl a$^+$ and BChl b$^+$ in CH_2Cl_2/CH_3OH solution (6:1). ^{14}N-spectra: T = 270 K, 20 mW microwave power, 200 W rf power (BChl a$^+$) and T = 220 K, 80 mW microwave power, 300 M rf power (BChl b$^+$). ^{1}H-special TRIPLE spectra: T = 220 K, total rf power 200 W, microwave power 20 mW (BChl a$^+$) and 80 mW (BChl b$^+$).

noticeable difference between the linewidth in liquid (ΔB = 1.26 ± 0.02 mT) and frozen solution (ΔB = 1.35 ± 0.02 mT). This must be due to g and/or hyperfine anisotropy. The observed EPR linewidth in frozen solution is in agreement with values reported earlier [19].

Liquid solution ^{14}N ENDOR and proton special TRIPLE spectra of BChl b$^+$ and BChl a$^+$ are shown in fig. 3. In the special TRIPLE experiment the high- and low-frequency NMR transitions of a particular nucleus are irradiated simultaneously. Thereby the signal intensity and the resolution can be increased as compared with an ENDOR experiment. The frequency axis gives the deviation from the proton Larmor frequency which is equivalent to one-half of the respective hyperfine coupling constant (hfc) [23, 24].

Ten proton lines and three ^{14}N lines are resolved in the spectra. The corresponding hfcs are listed in table 1.

An assignment of the hfcs to molecular positions in BChl b$^+$ can be accomplished on the basis of experimental evidence and/or by comparison with MO calculations. It is well known that ENDOR line intensities do not directly reflect the number of contributing nuclei because the individual nuclear relaxation behaviour determines the line intensity to a large extent [23,29]. This causes assignment problems which can often be overcome by applying the special TRIPLE resonance technique where the line intensities do reflect the number of contributing nuclei provided the electronic relaxation rates dominate the nuclear relaxation rates [23,24]. For photosynthetic pigments this was demonstrated in the special TRIPLE spectra of bacteriochlorophyll a, chlorophyll a and their pheophytin a radical anions [30–33]. In the proton special TRIPLE spectrum of BChl b$^+$ the three intense lines (corresponding hfcs: 4.70, 8.95 and 9.70 MHz) can therefore be assigned to the methyl protons at positions 1a, 4b and 5a (fig. 1).

Further aid in the assignment is provided by the signs of the hfcs because — for positive carbon π-spin densities — positive hfcs are expected for β-protons and negative hfcs for α-protons (for the characterization of β- and α-protons see ref. [34]). Relative signs of the hfcs can be obtained applying the general TRIPLE resonance technique where a particular NMR transition is pumped with a second strong unmodu-

Table 1

Hyperfine coupling constants (hfcs) in MHz of BChl a^{+} and BChl b^{+}. Experimental hfcs derived from ENDOR/TRIPLE in liquid solution, signs obtained from general TRIPLE resonance (see text). Theoretical values derived from MO calculations (see text)

Nucleus	Position [c]	BChl a^{+} [a]		BChl b^{+} [b]	
		exp. hfc	theoret. hfc [d]	exp. hfc	theoret. hfc [d]
β-H	3	+13.47	+13.93	+12.45	+14.67
	4	+16.35	+16.31	−	−
	7	+13.11	+13.79	+11.60	+14.16
	8	+11.76	+12.79	+10.55	+13.00
CH_3	1a	+4.93	+3.73	+4.70	+3.60
	4b		+0.13	+8.95	+6.46
	5a	+9.62	+7.32	+9.70	+6.91
α-H	4a	−0.55	−0.52	−8.02	−4.22
	α	+2.35	+1.61	+2.50	+1.43
	β	{ +1.30 }	+0.91	{ 1.20 [e] }	+0.83
	δ		+1.35		+1.23
other	10	−1.64	−2.80		−2.74
H	2b	−0.15	−0.26	{ 1,20 [e] }	−0.29
	3a		−0.87		−0.82
	7a	{ −0.55 }	−1.13	{ 0.40 [e] }	−1.53
	8a		−0.81		−0.82
^{14}N	I	−2.35 [f]	−1.84	2.3	−1.68
	II	−3.17	−2.32	3.3	−2.22
	III	−2.35 [f]	−2.20	2.3	−2.07
	IV	−3.05	−2.31	3.0	−2.11

[a] T = 220 K for protons (22, 33), T = 270 K for nitrogens.

[b] T = 220 K for protons and nitrogens.

[c] See molecular structure fig. 1. Note different substituents at positions 4a and 4b in BChl a and BChl b. For BChl a^{+} the groups of β-Hs at positions 3, 4, 7, 8, of CH_3 protons at positions 1a, 5a and of Hs in positions 2b, 3a, 4a, 7a and 8a, have been assigned by selective deuteration. The proton at position 10 was identified by proton/deuteron exchange experiments [22,27]. Specific assignments within these groups of protons are based on comparison with the calculations.

[d] RHF-INDO/SP method, Q factors relating s-spin densities and isotropic hfcs (MHz), see fig. 4.

[e] No signs could be determined for these hfcs because several protons having hfcs of almost identical magnitude but with different signs contribute to the corresponding ENDOR lines.

[f] Two nitrogens must be assigned to this hfc as shown by ^{15}N-ENDOR experiments [28].

lated rf field while recording the ENDOR spectrum [23]. Depending on the relative signs of the hfcs, changes of the signal intensities relative to the normal ENDOR spectrum are detected [23]. Using this technique we obtained a negative sign only for the hfc of 8.02 MHz, the large methyl hfcs taken as positive. This differs from our results for BChl a^{+} where no large negative hfc was observed. We therefore assign this hfc to the α-proton of the ethylidene group at ring II (position 4a, fig. 1). From a comparison with BChl a^{+} [22,27] the three largest positive proton hfcs are attributed to the β-protons at rings II and IV

(positions 3, 7 and 8, fig. 1).

The assignment of the three small proton hfcs (0.4, 1.2 and 2.5 MHz) given in table 1 is solely based on MO calculations. For BChl a^{+} we could achieve a definite assignment also for the small hfcs by isotopic labelling and proton/deuteron exchange experiments [22,27].

The instability of BChl b and its radical cation was a serious problem for our experiments. To ensure that no decomposition products gave rise to additional ENDOR or TRIPLE lines, general TRIPLE resonance was used. In this experiment changes of

line intensities are expected only for those ENDOR lines stemming from one particular paramagnetic species [21,23]. We observed significant general TRIPLE effects for all proton ENDOR lines of our BChl b$^+$ spectrum except for those corresponding to the two smallest proton hfcs (0.4 and 1.2 MHz). Several protons having positive and negative signs of their hfcs might, however, contribute to these two lines in which case the overall TRIPLE effect would vanish. The MO calculations predict indeed eight proton hfcs in the range between +1.5 and −2.7 MHz (see table 1). Furthermore, a paramagnetic decomposition product of BChl b is expected to have not only two such small proton hfcs.

Using an excess of ZnTPP$^+$ClO$_4^-$ for oxidizing BChl b we could, in the presence of light and traces of oxygen, obtain such a paramagnetic decomposition product having an EPR linewidth $\Delta B \approx 0.9$ mT. This product has been attributed earlier to a chlorin derivative with a structure similar to chlorophyll a [19]. The special TRIPLE spectrum obtained from this species was indeed very similar to that of the plant chlorophyll a radical cation [22,35], and none of the observed lines were coincident with those of BChl b$^+$. This product was, however, not observed when light, oxygen and an excess of ZnTPP$^+$ClO$_4^-$ were rigorously excluded.

The similarity of the hfcs found for BChl b$^+$ with those of BChl a$^+$, the occurrence of an additional methyl proton line and, in particular, the large negative hfc (−8.02 MHz), which is also predicted by the MO calculations, make it very probable that the observed spectra really arise from the BChl b radical cation.

We have also detected three ^{14}N ENDOR lines for BChl b$^+$ (fig. 3). The absolute values of the corresponding hfcs are again very similar to those of BChl a$^+$ (see table 1). Their signs could, however, not be determined due to the rather poor signal-to-noise ratio. In analogy to BChl a$^+$, two ^{14}N nuclei may be assigned to the smallest hfc (for BChl a$^+$ this has been verified by ^{15}N-ENDOR [28]).

The four proton hfcs found in earlier ENDOR experiments on BChl b$^+$ in frozen solution (1.12, 4.76, 8.96 and 12.88 MHz [19]) agree satisfactorily with some of our hfcs measured in liquid solution. However, our assignment, based on TRIPLE experiments, sign determination and comparison with advanced
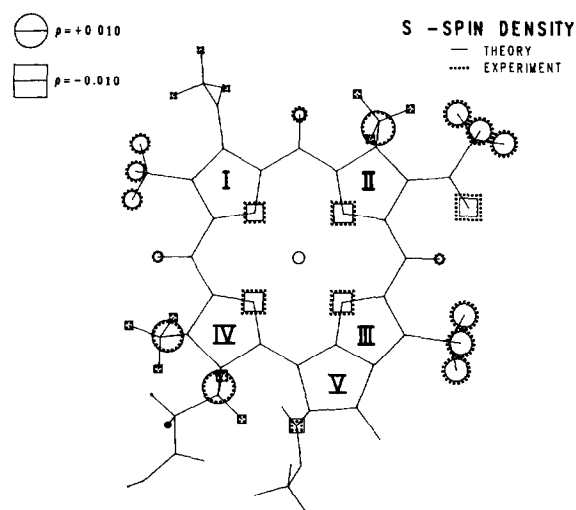

Fig. 4. Comparison of experimental (dotted) and calculated (solid lines) s-spin densities ρ for the BChl b radical cation. Their values are proportional to the area of the squares ($\rho < 0$) and circles ($\rho > 0$), respectively. For the calculation the RHF INDO/SP method was used (see text). The full molecular structure was taken except for a truncation of the isoprenoid chain R at position O-5 (fig. 1) [15]. Mostly standard bond lengths and angles were employed [15], atomic positions for ring V, the methyl groups (rings I and III), the acetyl group (ring I) and the ethylidene group (ring II) were determined by energy minimization. Thereby the acetyl group (ring I) was found to be 105° out-of-plane (dihedral angle with respect to positions C-1, C-2, C-2a and O-6, see fig. 1) due to steric hindrance. The ethylidene group (ring II) stayed approximately in the plane of the porphyrin system in spite of steric hindrance, because of the double bond between carbon positions 4 and 4a. Experimental values from isotropic hfcs (table 1) by use of: $Q(\text{H}) = 1420$ MHz, $Q(^{14}\text{N}) = 663$ MHz [15].

MO calculations, is different. The absolute value of the hfc of the ethylidene α-proton (4a, fig. 1) is much larger (−8.02 MHz) than was assumed in the earlier work (−4.8 MHz). Furthermore, the β-protons at rings II and IV (pos. 3, 7 and 8, fig. 1) have hfcs of only 10.55, 11.6, and 12.45 MHz. There are no proton hfcs as large as 16.8 MHz in BChl b$^+$, as was assumed in [19] to account for the EPR linewidth. The observed difference between the EPR linewidth of BChl b$^+$ in liquid and frozen solution (fig. 2) is probably mainly caused by the anisotropy of the large α-proton hfc at position 4a which gives rise to line broadening in randomly oriented rigid samples. With the hfcs and assignments given in table 1 the EPR spectrum of BChl

b^+ in liquid solution could be perfectly simulated (fig. 2, dotted line).

Comparing the corresponding hfcs of BChl b^+ and BChl a^+ (table 1) one finds almost no change for the methyl protons 1a and 5a (fig. 1). The couplings of the β-protons of rings II and IV [3,7,8] are reduced by only 10%, and in the region of small proton hfcs ($|a| < 2.5$ MHz) some ENDOR lines may have merged together so that for BChl b^+ only three proton hfcs are observed in this region. The major difference arises from the ethylidene substituent at ring II in BChl b^+, which obviously carries large π-spin density. For the α-proton (4a) and for the methyl protons (4b) comparable large hfcs are observed. The detailed picture of the spin density distribution reveals a close similarity of the highest occupied orbitals of BChl a^+ and BChl b^+ (see table 1).

The magnitudes and spectral assignments of the hfcs are in good agreement with predictions from our MO calculations [15] presented in table 1. Fig. 4 shows a graphical comparison between calculated and experimental s-spin densities. The agreement between experimental and calculated results is better than that reported earlier for bacteriochlorophyll radicals [19, 36–38] using other MO methods like PPP [39] or an "ab initio" molecular fragment method [40] which only calculate π-spin densities.

The investigation of the primary electron donor radical cation P_{960}^+ in the BChl b containing bacterium *Rps. viridis* is of special interest for the following reasons: The X-ray structure analysis of RC single crystals of this species clearly reveals P_{960} as a BChl b dimer [8]. However, the EPR linewidth of P_{960}^+ is not narrowed by the factor $2^{-1/2}$ as compared to that of the monomer BChl b^+. This is in contrast to the findings for the BChl a systems [9,10], where this narrowing of the linewidth by $2^{-1/2}$ has been explained by an *equal sharing* of the unpaired electron between two BChl a molecules [9]. This interpretation has been supported by ENDOR experiments on the primary donor P_{860}^+ in liquid and frozen solutions [10–14].

Recently, we have started ENDOR experiments on P_{960}^+ in liquid solution [16] which suggests an *unequal sharing* of the unpaired electron between the dimer halves. To support this idea, an unambiguous assignment of at least some of the signals will be necessary, e.g., from specifically dueterated RCs. Work along these lines is in progress.

References

[1] M.Y. Okamura, G. Feher and N. Nelson, in: Photosynthesis: energy conversion by plants and bacteria, Vol. 1, ed. Govindjee (Academic Press, New York, 1982) p. 195.

[2] F.K. Fong, Light reaction path of photosynthesis (Springer, Berlin, 1982).

[3] G. Feher and M.Y. Okamura, in: The photosynthetic bacteria, eds. R.K. Clayton and W.R. Sistrom (Plenum Press, New York, 1978) p. 349.

[4] B. Chance, D. DeVault, H. Frauenfelder, R.A. Marcus, J.R. Schrieffer and N. Sutin, eds., Tunneling in biological systems (Academic Press, New York, 1979).

[5] A.J. Hoff, Phys. Rept. 54 (1979) 75.

[6] A.J. Hoff, Biophys. Struct. Mech. 8 (1982) 107.

[7] H. Michel, J. Mol. Biol. 158 (1982) 567.

[8] J. Deisenhofer, O. Epp, K. Miki, R. Huber and H. Michel, J. Mol. Biol. 180 (1984) 385.

[9] J.R. Norris, R.A. Uphaus, H.L. Crespi and J.J. Katz, Proc. Natl. Acad. Sci. US 68 (1971) 625.

[10] G. Feher, A.J. Hoff, R.A. Isaacson and C.C. Ackerson, Ann. NY Acad. Sci. 244 (1975) 239.

[11] J.R. Norris, H. Scheer, M.E. Druyan and J.J. Katz, Proc. Natl. Acad. Sci. US 71 (1974) 4897.

[12] F. Lendzian, W. Lubitz, H. Scheer, C. Bubenzer and K. Möbius, J. Am. Chem. Soc. 103 (1981) 4635.

[13] W. Lubitz, F. Lendzian, H. Scheer, M. Plato and K. Möbius, in: Photochemistry and photobiology, Proceedings of the International Conference, University of Alexandria, Egypt, ed. A.H. Zewail (Harwood, New York, 1983) p. 1057.

[14] W. Lubitz, F. Lendzian, H. Scheer, J. Gottstein, M. Plato and K. Möbius, Proc. Natl. Acad. Sci. US 81 (1984) 1401.

[15] M. Plato, E. Tränkle, W. Lubitz, F. Lendzian and K. Möbius, Chem. Phys., submitted for publication.

[16] W. Lubitz, F. Lendzian, M. Plato, K. Möbius and E. Tränkle, in: Antennas and reaction centers of photosynthetic bacteria – structure, interactions and dynamics, ed. M.E. Michel-Beyerle (Springer, Berlin, 1985) p. 164.

[17] R. Steiner, Ph.D. Thesis, Botanisches Institut, Universität München, Munich (1984).

[18] R. Steiner, E. Cmiel and H. Scheer, Z. Naturforsch. 38c (1983) 748.

[19] M.S. Davis, A. Forman, L.K. Hanson, J.P. Thornber and J. Fajer, J. Phys. Chém. 83 (1979) 3325.

[20] H.H. Strain and W.A. Svec, in: The chlorophylls, eds. L.P. Vernor and G.R. Seely (Academic Press, New York, 1966).

[21] K. Möbius, M. Plato and W. Lubitz, Phys. Rept. 87 (1982) 171.

[22] F. Lendzian, Ph.D. Thesis, Department of Physics, Freie Universität Berlin, Berlin (1982).

[23] K. Möbius and R. Biehl, in: Multiple electron resonance spectroscopy, eds. M.M. Dorio and J.H. Freed (Plenum Press, New York, 1979) p. 475.

[24] K.P. Dinse, R. Biehl and K. Möbius, J. Chem. Phys. 61 (1974) 4335.

[25] M.J.S. Dewar, J.A. Hashmall and C.G. Venier, J. Am. Chem. Soc. 90 (1968) 1953.

[26] J.A. Pople and D.L. Beveridge, Approximate molecular orbital theory (McGraw-Hill, New York, 1970).

[27] W. Lubitz, F. Lendzian, M. Plato, H. Scheer and K. Möbius, to be published.

[28] W. Lubitz, R.A. Isaacson, E.C. Abresch and G. Feher, Proc. Natl. Acad. Sci. US 81 (1984) 7792.

[29] M. Plato, W. Lubitz and K. Möbius, J. Phys. Chem. 85 (1981) 1202.

[30] W. Lubitz, F. Lendzian and K. Möbius, Chem. Phys. Letters 81 (1981) 235.

[31] W. Lubitz, F. Lendzian and K. Möbius, Chem. Phys. Letters 84 (1981) 33.

[32] A.J. Hoff, F. Lendzian, K. Möbius and W. Lubitz, Chem. Phys. Letters 85 (1982) 3.

[33] F. Lendzian, W. Lubitz and K. Möbius, Chem. Phys. Letters 90 (1982) 375.

[34] A. Carrington and A.D. McLachlan, Introduction to magnetic resonance (Harper and Row, New York, 1969).

[35] M. Huber, F. Lendzian, W. Lubitz, E. Tränkle and K. Möbius, Chem. Phys. Letters, to be published.

[36] J. Fajer, A. Forman, M.S. Davis, L.D. Spaulding, D.C. Brune and R.H. Felton, J. Am. Chem. Soc. 99 (1977) 4134.

[37] J.D. Petke, G.M. Maggiora, L.L. Shipman and R.E. Christoffersen, Photochem. Photobiol. 33 (1981) 663.

[38] J.D. Petke, G.M. Maggiora, L.L. Shipman and R.E. Christoffersen, Photochem. Photobiol. 31 (1980) 243.

[39] R. Pariser and R.G. Parr, J. Chem. Phys. 21 (1953) 466.

[40] R.E. Christoffersen, D.W. Genson and G.M. Maggiora, J. Chem. Phys. 54 (1971) 239.